

Gluon-Spin Contribution to the Proton Spin from the Double-Helicity Asymmetry in Inclusive π^0 Production in Polarized $p + p$ Collisions at $\sqrt{s} = 200$ GeV

A. Adare,¹² S. Afanasiev,²⁶ C. Aidala,³⁷ N. N. Ajitanand,⁵⁴ Y. Akiba,^{48,49} H. Al-Bataineh,⁴³ J. Alexander,⁵⁴ K. Aoki,^{31,48} L. Aphecetche,⁵⁶ J. Asai,⁴⁸ E. T. Atomssa,³² R. Averbeck,⁵⁵ T. C. Awes,⁴⁴ B. Azmoun,⁷ V. Babintsev,²² M. Bai,⁶ G. Baksay,¹⁸ L. Baksay,¹⁸ A. Baldisseri,¹⁵ K. N. Barish,⁸ P. D. Barnes,³⁴ B. Bassalleck,⁴² A. T. Basye,¹ S. Bathe,⁸ S. Batsouli,⁴⁴ V. Baublis,⁴⁷ C. Baumann,³⁸ A. Bazilevsky,⁷ S. Belikov,^{7,†} R. Bennett,⁵⁵ A. Berdnikov,⁵¹ Y. Berdnikov,⁵¹ A. A. Bickley,¹² J. G. Boissevain,³⁴ H. Borel,¹⁵ K. Boyle,⁵⁵ M. L. Brooks,³⁴ H. Buesching,⁷ V. Bumazhnov,²² G. Bunce,^{7,49} S. Butsyk,³⁴ C. M. Camacho,³⁴ S. Campbell,⁵⁵ P. Chand,⁴ B. S. Chang,⁶³ W. C. Chang,² J.-L. Charvet,¹⁵ S. Chernichenko,²² C. Y. Chi,¹³ M. Chiu,²³ I. J. Choi,⁶³ R. K. Choudhury,⁴ T. Chujo,⁵⁹ P. Chung,⁵⁴ A. Churnin,²² V. Cianciolo,⁴⁴ Z. Citron,⁵⁵ B. A. Cole,¹³ P. Constantin,³⁴ M. Csanád,¹⁷ T. Csörgő,²⁸ T. Dahms,⁵⁵ S. Dairaku,^{31,48} K. Das,¹⁹ G. David,⁷ A. Denisov,²² D. d'Enterria,³² A. Deshpande,^{49,55} E. J. Desmond,⁷ O. Dietzsch,⁵² A. Dion,⁵⁵ M. Donadelli,⁵² O. Drapier,³² A. Drees,⁵⁵ K. A. Drees,⁶ A. K. Dubey,⁶² A. Durum,²² D. Dutta,⁴ V. Dzordzhadze,⁸ Y. V. Efremenko,⁴⁴ J. Egdemir,⁵⁵ F. Ellinghaus,¹² T. Engelmore,¹³ A. Enokizono,³³ H. En'yo,^{48,49} S. Esumi,⁵⁹ K. O. Eyser,⁸ B. Fadem,³⁹ D. E. Fields,^{42,49} M. Finger,⁹ M. Finger, Jr.,⁹ F. Fleuret,³² S. L. Fokin,³⁰ Z. Fraenkel,^{62,†} J. E. Frantz,⁵⁵ A. Franz,⁷ A. D. Frawley,¹⁹ K. Fujiwara,⁴⁸ Y. Fukao,^{31,48} T. Fusayasu,⁴¹ I. Garishvili,⁵⁷ A. Glenn,¹² H. Gong,⁵⁵ M. Gonin,³² J. Gosset,¹⁵ Y. Goto,^{48,49} R. Granier de Cassagnac,³² N. Grau,¹³ S. V. Greene,⁶⁰ M. Grosse Perdekamp,^{23,49} T. Gunji,¹¹ H.-Å. Gustafsson,³⁶ A. Hadj Henni,⁵⁶ J. S. Haggerty,⁷ H. Hamagaki,¹¹ R. Han,⁴⁶ E. P. Hartouni,³³ K. Haruna,²¹ E. Haslum,³⁶ R. Hayano,¹¹ M. Heffner,³³ T. K. Hemmick,⁵⁵ T. Hester,⁸ X. He,²⁰ J. C. Hill,²⁵ M. Hohlmann,¹⁸ W. Holzmann,⁵⁴ K. Homma,²¹ B. Hong,²⁹ T. Horaguchi,^{11,48,58} D. Hornback,⁵⁷ S. Huang,⁶⁰ T. Ichihara,^{48,49} R. Ichimiya,⁴⁸ Y. Ikeda,⁵⁹ K. Imai,^{31,48} J. Imrek,¹⁶ M. Inaba,⁵⁹ D. Isenhower,¹ M. Ishihara,⁴⁸ T. Isobe,¹¹ M. Issah,⁵⁴ A. Isupov,²⁶ D. Ivanischev,⁴⁷ B. V. Jacak,^{55,*} J. Jia,¹³ J. Jin,¹³ B. M. Johnson,⁷ K. S. Joo,⁴⁰ D. Jouan,⁴⁵ F. Kajihara,¹¹ S. Kametani,⁴⁸ N. Kamihara,⁴⁹ J. Kamin,⁵⁵ J. H. Kang,⁶³ J. Kapustinsky,³⁴ D. Kawall,^{37,49} A. V. Kazantsev,³⁰ T. Kempel,²⁵ A. Khanzadeev,⁴⁷ K. M. Kijima,²¹ J. Kikuchi,⁶¹ B. I. Kim,²⁹ D. H. Kim,⁴⁰ D. J. Kim,⁶³ E. Kim,⁵³ S. H. Kim,⁶³ E. Kinney,¹² K. Kiriluk,¹² A. Kiss,¹⁷ E. Kistenev,⁷ J. Klay,³³ C. Klein-Boesing,³⁸ L. Kochenda,⁴⁷ V. Kochetkov,²² B. Komkov,⁴⁷ M. Konno,⁵⁹ J. Koster,²³ A. Kozlov,⁶² A. Král,¹⁴ A. Kravitz,¹³ G. J. Kunde,³⁴ K. Kurita,^{50,48} M. Kurosawa,⁴⁸ M. J. Kweon,²⁹ Y. Kwon,⁵⁷ G. S. Kyle,⁴³ R. Lacey,⁵⁴ Y. S. Lai,¹³ J. G. Lajoie,²⁵ D. Layton,²³ A. Lebedev,²⁵ D. M. Lee,³⁴ K. B. Lee,²⁹ T. Lee,⁵³ M. J. Leitch,³⁴ M. A. L. Leite,⁵² B. Lenzi,⁵² P. Liebing,⁴⁹ T. Liška,¹⁴ A. Litvinenko,²⁶ H. Liu,⁴³ M. X. Liu,³⁴ X. Li,¹⁰ B. Love,⁶⁰ D. Lynch,⁷ C. F. Maguire,⁶⁰ Y. I. Makdisi,⁶ A. Malakhov,²⁶ M. D. Malik,⁴² V. I. Manko,³⁰ E. Mannel,¹³ Y. Mao,^{46,48} L. Mašek,^{9,24} H. Masui,⁵⁹ F. Matathias,¹³ M. McCumber,⁵⁵ P. L. McGaughey,³⁴ N. Means,⁵⁵ B. Meredith,²³ Y. Miake,⁵⁹ P. Mikeš,²⁴ K. Miki,⁵⁹ A. Milov,⁷ M. Mishra,³ J. T. Mitchell,⁷ A. K. Mohanty,⁴ Y. Morino,¹¹ A. Morreale,⁸ D. P. Morrison,⁷ T. V. Moukhanova,³⁰ D. Mukhopadhyay,⁶⁰ J. Murata,^{50,48} S. Nagamiya,²⁷ J. L. Nagle,¹² M. Naglis,⁶² M. I. Nagy,¹⁷ I. Nakagawa,^{48,49} Y. Nakamiya,²¹ T. Nakamura,²¹ K. Nakano,^{48,58} J. Newby,³³ M. Nguyen,⁵⁵ T. Niita,⁵⁹ R. Nouicer,⁵ A. S. Nyanin,³⁰ E. O'Brien,⁷ S. X. Oda,¹¹ C. A. Ogilvie,²⁵ H. Okada,^{31,48} K. Okada,⁴⁹ M. Oka,⁵⁹ Y. Onuki,⁴⁸ A. Oskarsson,³⁶ M. Ouchida,²¹ K. Ozawa,¹¹ R. Pak,⁵ A. P. T. Palounek,³⁴ V. Pantuev,⁵⁵ V. Papavassiliou,⁴³ J. Park,⁵³ W. J. Park,²⁹ S. F. Pate,⁴³ H. Pei,²⁵ J.-C. Peng,²³ H. Pereira,¹⁵ V. Peresedov,²⁶ D. Yu. Peressounko,³⁰ C. Pinkenburg,⁷ M. L. Porschke,⁷ A. K. Purwar,³⁴ H. Qu,²⁰ J. Rak,⁴² A. Rakotozafindrabe,³² I. Ravinovich,⁶² K. F. Read,^{44,57} S. Rembeczki,¹⁸ M. Reuter,⁵⁵ K. Reygers,³⁸ V. Riabov,⁴⁷ Y. Riabov,⁴⁷ D. Roach,⁶⁰ G. Roche,³⁵ S. D. Rolnick,⁸ M. Rosati,²⁵ S. S. E. Rosendahl,³⁶ P. Rosnet,³⁵ P. Rukoyatkin,²⁶ P. Ružička,²⁴ V. L. Rykov,⁴⁸ B. Sahlmueller,³⁸ N. Saito,^{31,48,49} T. Sakaguchi,⁷ S. Sakai,⁵⁹ K. Sakashita,^{48,58} V. Samsonov,⁴⁷ T. Sato,⁵⁹ S. Sawada,²⁷ K. Sedgwick,⁸ J. Seele,¹² R. Seidl,²³ A. Yu. Semenov,²⁵ V. Semenov,²² R. Seto,⁸ D. Sharma,⁶² I. Shein,²² T.-A. Shibata,^{48,58} K. Shigaki,²¹ M. Shimomura,⁵⁹ K. Shoji,^{31,48} P. Shukla,⁴ A. Sickles,⁷ C. L. Silva,⁵² D. Silvermyr,⁴⁴ C. Silvestre,¹⁵ K. S. Sim,²⁹ B. K. Singh,³ C. P. Singh,³ V. Singh,³ M. Slunečka,⁹ A. Soldatov,²² R. A. Soltz,³³ W. E. Sondheim,³⁴ S. P. Sorensen,⁵⁷ I. V. Sourikova,⁷ F. Staley,¹⁵ P. W. Stankus,⁴⁴ E. Stenlund,³⁶ M. Stepanov,⁴³ A. Ster,²⁸ S. P. Stoll,⁷ T. Sugitate,²¹ C. Suire,⁴⁵ A. Sukhanov,⁵ J. Sziklai,²⁸ E. M. Takagui,⁵² A. Taketani,^{48,49} R. Tanabe,⁵⁹ Y. Tanaka,⁴¹ S. Taneja,⁵⁵ K. Tanida,^{48,49} M. J. Tannenbaum,⁷ A. Taranenko,⁵⁴ P. Tarján,¹⁶ H. Themann,⁵⁵ T. L. Thomas,⁴² M. Togawa,^{31,48} A. Toia,⁵⁵ L. Tomášek,²⁴ Y. Tomita,⁵⁹ H. Torii,^{21,48} R. S. Towell,¹ V.-N. Tram,³² I. Tserruya,⁶² Y. Tsuchimoto,²¹ C. Vale,²⁵ H. Valle,⁶⁰ H. W. van Hecke,³⁴ A. Veicht,²³ J. Velkovska,⁶⁰ R. Vertesi,¹⁶ A. A. Vinogradov,³⁰ M. Virius,¹⁴ V. Vrba,²⁴ E. Vznuzdaev,⁴⁷ D. Walker,⁵⁵ X. R. Wang,⁴³ Y. Watanabe,^{48,49} F. Wei,²⁵ J. Wessels,³⁸ S. N. White,⁷ S. Williamson,²³ D. Winter,¹³ C. L. Woody,⁷ M. Wysocki,¹² W. Xie,⁴⁹ Y. L. Yamaguchi,⁶¹ K. Yamaura,²¹ R. Yang,²³ A. Yanovich,²² J. Ying,²⁰ S. Yokkaichi,^{48,49}

G. R. Young,⁴⁴ I. Younus,⁴² I. E. Yushmanov,³⁰ W. A. Zajc,¹³ O. Zaudtke,³⁸ C. Zhang,⁴⁴
S. Zhou,¹⁰ and L. Zolin²⁶

(PHENIX Collaboration)

- ¹Abilene Christian University, Abilene, Texas 79699, USA
²Institute of Physics, Academia Sinica, Taipei 11529, Taiwan
³Department of Physics, Banaras Hindu University, Varanasi 221005, India
⁴Bhabha Atomic Research Centre, Bombay 400 085, India
⁵Chemistry Department, Brookhaven National Laboratory, Upton, New York 11973-5000, USA
⁶Collider-Accelerator Department, Brookhaven National Laboratory, Upton, New York 11973-5000, USA
⁷Physics Department, Brookhaven National Laboratory, Upton, New York 11973-5000, USA
⁸University of California - Riverside, Riverside, California 92521, USA
⁹Charles University, Ovocný trh 5, Praha 1, 116 36, Prague, Czech Republic
¹⁰China Institute of Atomic Energy (CIAE), Beijing, People's Republic of China
¹¹Center for Nuclear Study, Graduate School of Science, University of Tokyo, 7-3-1 Hongo, Bunkyo, Tokyo 113-0033, Japan
¹²University of Colorado, Boulder, Colorado 80309, USA
¹³Columbia University, New York, New York 10027 and Nevis Laboratories, Irvington, New York 10533, USA
¹⁴Czech Technical University, Zikova 4, 166 36 Prague 6, Czech Republic
¹⁵Dapnia, CEA Saclay, F-91191, Gif-sur-Yvette, France
¹⁶Debrecen University, H-4010 Debrecen, Egyetem tér 1, Hungary
¹⁷ELTE, Eötvös Loránd University, H - 1117 Budapest, Pázmány P. s. 1/A, Hungary
¹⁸Florida Institute of Technology, Melbourne, Florida 32901, USA
¹⁹Florida State University, Tallahassee, Florida 32306, USA
²⁰Georgia State University, Atlanta, Georgia 30303, USA
²¹Hiroshima University, Kagamiyama, Higashi-Hiroshima 739-8526, Japan
²²IHEP Protvino, State Research Center of Russian Federation, Institute for High Energy Physics, Protvino, 142281, Russia
²³University of Illinois at Urbana-Champaign, Urbana, Illinois 61801, USA
²⁴Institute of Physics, Academy of Sciences of the Czech Republic, Na Slovance 2, 182 21 Prague 8, Czech Republic
²⁵Iowa State University, Ames, Iowa 50011, USA
²⁶Joint Institute for Nuclear Research, 141980 Dubna, Moscow Region, Russia
²⁷KEK, High Energy Accelerator Research Organization, Tsukuba, Ibaraki 305-0801, Japan
²⁸KFKI Research Institute for Particle and Nuclear Physics of the Hungarian Academy of Sciences (MTA KFKI RMKI), H-1525 Budapest 114, POBox 49, Budapest, Hungary
²⁹Korea University, Seoul, 136-701, Korea
³⁰Russian Research Center "Kurchatov Institute", Moscow, Russia
³¹Kyoto University, Kyoto 606-8502, Japan
³²Laboratoire Leprince-Ringuet, Ecole Polytechnique, CNRS-IN2P3, Route de Saclay, F-91128, Palaiseau, France
³³Lawrence Livermore National Laboratory, Livermore, California 94550, USA
³⁴Los Alamos National Laboratory, Los Alamos, New Mexico 87545, USA
³⁵LPC, Université Blaise Pascal, CNRS-IN2P3, Clermont-Fd, 63177 Aubiere Cedex, France
³⁶Department of Physics, Lund University, Box 118, SE-221 00 Lund, Sweden
³⁷Department of Physics, University of Massachusetts, Amherst, Massachusetts 01003-9337, USA
³⁸Institut für Kernphysik, University of Muenster, D-48149 Muenster, Germany
³⁹Muhlenberg College, Allentown, Pennsylvania 18104-5586, USA
⁴⁰Myongji University, Yongin, Kyonggido 449-728, Korea
⁴¹Nagasaki Institute of Applied Science, Nagasaki-shi, Nagasaki 851-0193, Japan
⁴²University of New Mexico, Albuquerque, New Mexico 87131, USA
⁴³New Mexico State University, Las Cruces, New Mexico 88003, USA
⁴⁴Oak Ridge National Laboratory, Oak Ridge, Tennessee 37831, USA
⁴⁵IPN-Orsay, Université Paris Sud, CNRS-IN2P3, BP1, F-91406, Orsay, France
⁴⁶Peking University, Beijing, People's Republic of China
⁴⁷PNPI, Petersburg Nuclear Physics Institute, Gatchina, Leningrad region, 188300, Russia
⁴⁸RIKEN Nishina Center for Accelerator-Based Science, Wako, Saitama 351-0198, JAPAN
⁴⁹RIKEN BNL Research Center, Brookhaven National Laboratory, Upton, New York 11973-5000, USA
⁵⁰Physics Department, Rikkyo University, 3-34-1 Nishi-Ikebukuro, Toshima, Tokyo 171-8501, Japan
⁵¹Saint Petersburg State Polytechnic University, Saint Petersburg, Russia
⁵²Universidade de São Paulo, Instituto de Física, Caixa Postal 66318, São Paulo CEP05315-970, Brazil
⁵³System Electronics Laboratory, Seoul National University, Seoul, Korea
⁵⁴Chemistry Department, Stony Brook University, Stony Brook, SUNY, New York 11794-3400, USA

⁵⁵Department of Physics and Astronomy, Stony Brook University, SUNY, Stony Brook, New York 11794, USA.

⁵⁶SUBATECH (Ecole des Mines de Nantes, CNRS-IN2P3, Université de Nantes) BP 20722 - 44307, Nantes, France

⁵⁷University of Tennessee, Knoxville, Tennessee 37996, USA

⁵⁸Department of Physics, Tokyo Institute of Technology, Oh-okayama, Meguro, Tokyo 152-8551, Japan

⁵⁹Institute of Physics, University of Tsukuba, Tsukuba, Ibaraki 305, Japan

⁶⁰Vanderbilt University, Nashville, Tennessee 37235, USA

⁶¹Waseda University, Advanced Research Institute for Science and Engineering, 17 Kikui-cho, Shinjuku-ku, Tokyo 162-0044, Japan

⁶²Weizmann Institute, Rehovot 76100, Israel

⁶³Yonsei University, IPAP, Seoul 120-749, Korea

(Received 6 October 2008; published 1 July 2009)

The double helicity asymmetry in neutral pion production for $p_T = 1$ to 12 GeV/ c was measured with the PHENIX experiment to access the gluon-spin contribution, ΔG , to the proton spin. Measured asymmetries are consistent with zero, and at a theory scale of $\mu^2 = 4$ GeV² a next to leading order QCD analysis gives $\Delta G^{[0.02,0.3]} = 0.2$, with a constraint of $-0.7 < \Delta G^{[0.02,0.3]} < 0.5$ at $\Delta\chi^2 = 9$ ($\sim 3\sigma$) for the sampled gluon momentum fraction (x) range, 0.02 to 0.3. The results are obtained using predictions for the measured asymmetries generated from four representative fits to polarized deep inelastic scattering data. We also consider the dependence of the ΔG constraint on the choice of the theoretical scale, a dominant uncertainty in these predictions.

DOI: 10.1103/PhysRevLett.103.012003

PACS numbers: 13.88.+e, 13.85.Ni, 21.10.Hw, 25.40.Ep

The originally surprising observations [1–3] that the quark spin contribution to the proton spin is only $\sim 25\%$ indicate that the majority of the proton spin on average comes from the gluon-spin contribution, ΔG , and/or from gluon and quark orbital angular momentum. High energy polarized $p + p$ collisions at the Relativistic Heavy Ion Collider (RHIC) at Brookhaven National Laboratory access ΔG through spin-dependent gluon-gluon (gg) and quark-gluon (qg) scattering.

This Letter presents results from the 2006 RHIC run on ΔG from measurements by the PHENIX experiment of the double-helicity asymmetry (A_{LL}) in inclusive midrapidity π^0 production. ΔG can be extracted from $A_{LL}^{\pi^0}$ using next-to-leading order (NLO) perturbative quantum chromodynamics (pQCD) [4], which successfully describes unpolarized cross sections measured at RHIC for many inclusive processes [5–7], including midrapidity π^0 production [8], at $\sqrt{s} = 200$ GeV. These $A_{LL}^{\pi^0}$ data represent a factor of 2 improvement in the statistical uncertainty compared to previous results [8–10]. The data significantly constrain ΔG , as presented in a recent global fit (DSSV) [11] of both RHIC and polarized deep inelastic scattering (pDIS) data, which used a preliminary version of these results. We further present the impact of experimental systematic and two theoretical uncertainties on our determination of ΔG .

We define $\Delta G^{[a,b]}(\mu^2) \equiv \int_a^b dx \Delta g(x, \mu^2)$, with $\Delta g(x, \mu^2)$, the polarized gluon distribution, a function of x , the gluon momentum fraction, and μ^2 , the factorization scale. Thus $\Delta G^{[0,1]} \equiv \Delta G$. Figure 1(a) shows the best fit (BF) $\Delta g(x)$ from four NLO pDIS fits (in the \overline{MS} scheme): GRSV-std [12], BB (“ISET-4”) [13], LSS [14], and GS-C [15] which assumes a node, or sign change, in $\Delta g(x)$. As the pDIS data have limited sensitivity to ΔG , there remains large uncertainty. Table I lists $\Delta G^{[a,b]}$ for two x ranges.

We define $A_{LL}^{\pi^0} = (\sigma_{++} - \sigma_{+-})/(\sigma_{++} + \sigma_{+-})$, with σ_{++} (σ_{+-}) the beam helicity dependent differential cross sections for inclusive π^0 production from collisions of longitudinally polarized protons with the same (opposite) helicity. The asymmetry is measured using

$$A_{LL}^{\pi^0} = \frac{1}{\langle P_B P_Y \rangle} \frac{N_{++} - RN_{+-}}{N_{++} + RN_{+-}}, \quad R = \frac{L_{++}}{L_{+-}} \quad (1)$$

where P_B and P_Y are the polarizations of the two RHIC beams, called “blue” and “yellow,” and R , the relative luminosity, is the ratio of integrated luminosities (L) for the same and opposite helicity collisions. Here we take N to be the π^0 yield in a transverse momentum (p_T) bin.

Each π^0 p_T bin is sensitive to a broad range in gluon x . Figure 1(b) shows the π^0 yield as a function of gluon x for

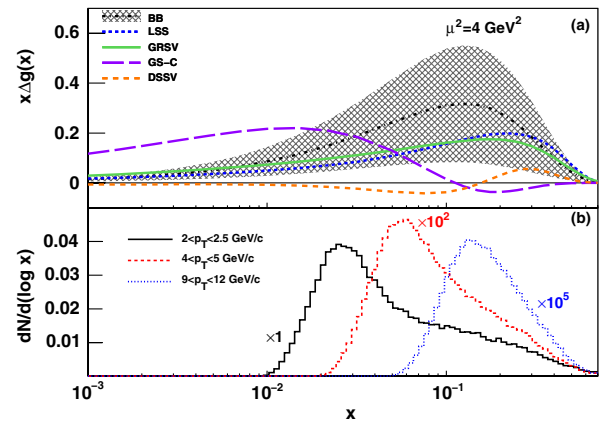


FIG. 1 (color online). (a) The polarized gluon distribution as a function of x for five fits to polarized data. The hatched band is pDIS uncertainty (BB). (b) π^0 yield as a function of gluon x in three π^0 p_T bins from an NLO pQCD simulation.

TABLE I. $\Delta G^{[a,b]}$ at $\mu^2 = 4 \text{ GeV}^2$ for each group's best fit and the χ^2 when comparing the expected A_{LL} in Fig. 3(a) with the data (8 degrees of freedom). Also shown are the minimum χ^2 and corresponding $\Delta G^{[0.02,0.3]}$ found in Fig. 3(b).

Group	Published best fit		χ^2	From Fig. 3(b)	
	$\Delta G^{[0,1]}$	$\Delta G^{[0.02,0.3]}$		$\Delta G^{[0.02,0.3]}$	χ^2
GS-C	0.95	0.18	8.3	0.1	8.5
DSSV	-0.05	-0.03	7.5
LSS	0.60	0.37	22.4	0.2	7.0
GRSV	0.67	0.38	14.8	0.2	7.1
BB	0.93	0.67	69.0	0.2	7.2

three $A_{LL}^{\pi^0}$ p_T bins from a NLO pQCD simulation [4,16]. They are peaked at $x_T/0.7$ [17], with $x_T \equiv p_T/(\sqrt{s}/2)$. The x ranges overlap, with the data covering primarily the range $0.02 < x < 0.3$, and so we probe $\Delta G^{[0.02,0.3]}$.

The highly segmented PHENIX electromagnetic calorimeter (EMCal) [18] is used to detect $\pi^0 \rightarrow \gamma\gamma$ decays. The EMCal covers a pseudorapidity range of $|\eta| < 0.35$ and azimuthal angle range of $\Delta\phi = \pi$, with segmentation $\Delta\eta \times \Delta\phi = 0.01 \times 0.01$. We required for each of the two decay photons an energy deposition pattern consistent with an electromagnetic shower, no charged track pointing to the location of the deposited energy, and standard quality assurance requirements [9]. Events were obtained from an EMCal based high p_T photon trigger [19] in coincidence with a minimum bias trigger [8] (also used to obtain the relative luminosity). The EMCal based trigger efficiency for π^0 was 5% at $p_T \approx 1 \text{ GeV}/c$ and plateaued at 90% for $p_T > 3.5 \text{ GeV}/c$. The minimum bias trigger was defined as the coincidence of signals from forward and backward beam-beam counters (BBC) with full azimuthal coverage located at pseudorapidities $\pm(3.0-3.9)$ [20]. The analyzed data sample corresponded to an integrated luminosity of 6.5 pb^{-1} .

Each collider ring of RHIC was filled with up to 111 out of a possible 120 bunches, spaced 106 ns apart, with bunch helicities set such that all four beam helicity combinations occurred in sequences of four bunch crossings. The pattern of helicity combinations for each RHIC fill (typically 8 hrs) was cycled between four possibilities to reduce systematic uncertainties that could be correlated to the bunch structure in RHIC [8]. Events were tagged with the bunch crossing number to obtain the beam helicities for the event. The luminosity weighted beam polarization product was $\langle P_B P_Y \rangle = 0.322 \pm 0.027$ (8.3%), with single beam polarizations of 0.560 and 0.575. Small nonzero transverse single spin asymmetries in very forward neutron production [8,21] were measured for each beam. The fill-by-fill ratio of this asymmetry to the beam polarization was constant within statistical uncertainties, confirming the polarization direction stability at PHENIX and the spin sign identification of the recorded collisions. The polarization vector was found to be 99% aligned with the beam (momentum) axis.

As in our previous analyses [8,9], the relative luminosity ratio R was obtained from crossing-by-crossing collected minimum bias (BBC) trigger counts, which measure about half of the $p + p$ inelastic cross section [19]. The uncertainty on R was derived from the comparison with a second trigger based on the zero degree calorimeters [22], which count very forward, energetic neutrals, and so is sensitive to different physics processes with a different angular acceptance than the BBC. It contributed a p_T independent systematic uncertainty to A_{LL} of 7×10^{-4} .

Equation (1) is used to determine, on a fill-by-fill basis, A_{LL} for the yield in the π^0 mass peak (112–162 MeV/c^2) for each p_T bin. The asymmetries were averaged over fills and corrected for the asymmetry in the background contribution (determined from two 50 MeV/c^2 wide sidebands on either side of the π^0 peak) [9], which was consistent with zero.

Figure 2(a) shows the measured $A_{LL}^{\pi^0}$ in comparison with our published data from the 2005 RHIC run [8]. The results are found to be statistically consistent with a 13% confidence level. The inset shows an expanded view of the low p_T region, as well as the relative luminosity uncertainty. Besides this and the scale uncertainty from polarization, other systematic uncertainties that can be found by using a bunch polarization sign randomization technique [9] appear negligible. In addition, the results were robust against variation of the π^0 identification criteria. The parity-violating single helicity asymmetry A_L was measured for each beam, and was consistent with zero within statistical uncertainty for all p_T bins.

Also shown in Fig. 2(a) are NLO pQCD predictions (assuming $\mu = p_T$) of $A_{LL}^{\pi^0}$ [4] based on fits of pDIS data by GRSV with three values for ΔG at the *input* scale of $\mu^2 = 0.4 \text{ GeV}^2$: (1) “std,” their best fit value with $\Delta G = 0.24$, (2) $\Delta G = 0$, and (3) $\Delta G = -1.05$. The results are most consistent with GRSV $\Delta G = 0$. CTEQ6 unpolarized parton distribution functions [23] and DSS fragmentation functions [24] were used in all calculations. Using alternative parton distribution functions [25] or fragmentation functions [26] did not lead to significant differences in the A_{LL} expectations.

A_{LL} expectations were calculated [4] based on refits to the pDIS data with a range of inputs for $\Delta G^{[0,1]}$ at

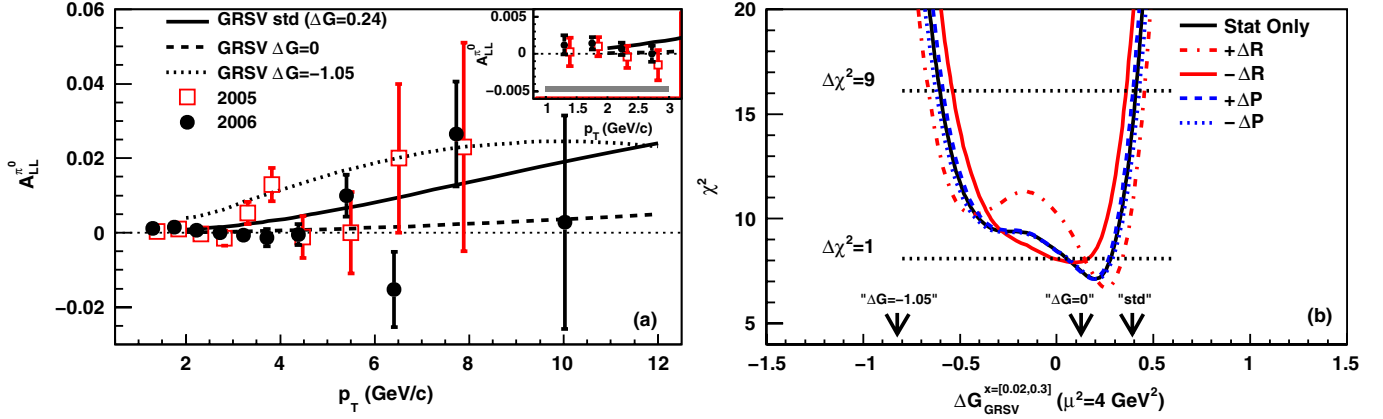


FIG. 2 (color online). (a) Asymmetry in π^0 production as a function of p_T . The error bars are statistical uncertainties. An 8.3% scale uncertainty due to the uncertainty in beam polarization is not shown. The p_T independent uncertainty of 7×10^{-4} due to relative luminosity is shown only in the inset as a shaded bar. For comparison, we also show our 2005 result. NLO pQCD expectations based on several inputs for ΔG in the GRSV parametrization are plotted. (b) The χ^2 profile as a function of $\Delta G_{\text{GRSV}}^{[0.02,0.3]}$ using the combined 2005 and 2006 data considering only statistical uncertainty, or also varying by $\pm 1\sigma$ the two primary experimental systematic uncertainties, from beam polarizations ($\pm \Delta P$) and relative luminosity ($\pm \Delta R$).

$\mu^2 = 0.4 \text{ GeV}^2$ in the GRSV parametrization. Similar to our previous analysis [8], χ^2 values were calculated using our combined 2005 and 2006 data for these expectations. In Fig. 2(b), these values are plotted as a function of $\Delta G^{[0.02,0.3]}$ evolved to $\mu^2 = 4 \text{ GeV}^2$. We previously estimated the nonperturbative contribution to be small for $p_T > 2 \text{ GeV}/c$ [8], and so use this as a minimum cutoff in this analysis. The solid curve shows the result considering only statistical uncertainties.

The quadratic ΔG contribution from gg interactions in $p + p$ collisions leads to two minima in Fig. 2(b), while the linear ΔG contribution from qg interactions breaks the symmetry in these minima [4,8]. The χ^2 profile is thus not parabolic, and so we show $\Delta\chi^2 \equiv \chi^2 - \chi^2_{\text{min}} = 1$ and 9 corresponding to “1 σ ” and “3 σ ” uncertainties.

The effects of the two largest experimental systematic uncertainties, due to polarization and relative luminosity, are shown in Fig. 2(b). The polarization uncertainty is insignificant when extracting ΔG . However, the uncertainty on relative luminosity, though small, cannot be neglected. Accounting for statistical uncertainty, we find $\Delta G_{\text{GRSV}}^{[0.02,0.3]} = 0.2 \pm 0.1$ (1σ) and $0.2^{+0.2}_{-0.8}$ (3σ) with an additional experimental systematic uncertainty of ± 0.1 .

Figure 3(a) shows $A_{\text{LL}}^{\pi^0}$ expectations [4,16] based on the parametrizations discussed above, along with the pDIS uncertainty on $\Delta g(x)$ in BB propagated to A_{LL} . The χ^2 values for comparing each curve with the data are given in Table I. The three fit results without a node in $\Delta g(x)$ —LSS, GRSV and BB—have large values of $\Delta G^{[0.02,0.3]}$ which lead to relatively large asymmetries that lie mostly above the data, though they are consistent within the large uncertainty from pDIS. For GS-C and DSSV, which have a node in $\Delta g(x)$ near the center of the sampled x region, a cancellation between the positive and negative contribution in

the wide x distribution in each p_T bin leads to a small value of $\Delta G^{[0.02,0.3]}$ and thus small A_{LL} .

To investigate if there is any consistent constraint on $\Delta G^{[0.02,0.3]}$, independent of the parametrization choice, the χ^2 profiles in Fig. 3(b) were calculated based on the pDIS fit results in Fig. 1(a) (excluding DSSV). New polarized gluon distributions were produced using $\Delta g(x) = \lambda \Delta g_{\text{BF}}(x)$ at the input scale, with $\Delta g_{\text{BF}}(x)$ the *best fit* result. For each parametrization, a family of A_{LL} curves were generated by varying λ , i.e., varying $\Delta G^{[0,1]}$ while fixing both the quark helicity distributions and the shape of $\Delta g(x)$ to the best fit values. This approach differs from that of Fig. 2(b), where both the quark helicity distributions and

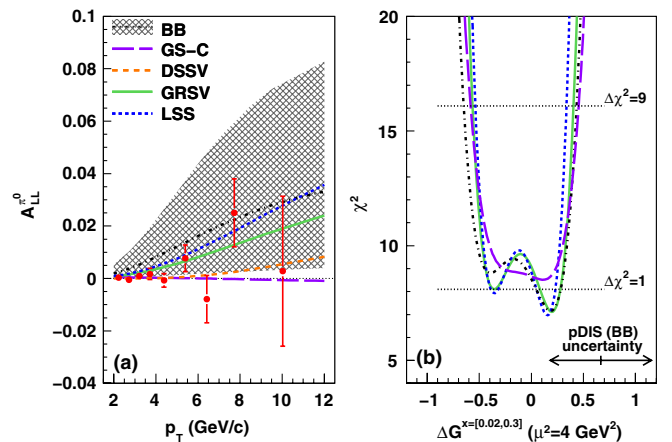


FIG. 3 (color online). (a) π^0 asymmetry expectations for different $\Delta g(x)$ in Fig. 1(b). The hatched band is the pDIS uncertainty (BB). Combined 2005 and 2006 data are also plotted (statistical errors only). (b) The χ^2 profile as a function of $\Delta G_{\text{GRSV}}^{[0.02,0.3]}$ for the same parametrizations. Arrows indicate uncertainty on the BB best fit. $\Delta\chi^2$ values are shown for GRSV.

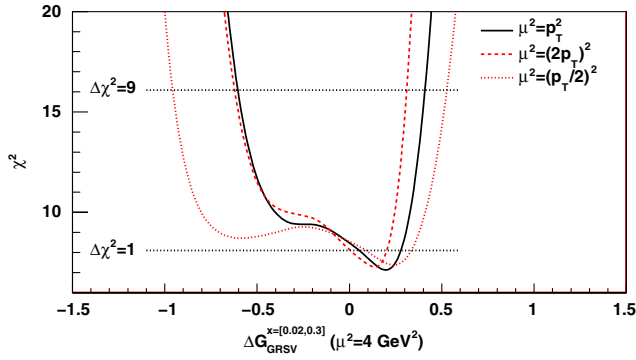


FIG. 4 (color online). χ^2 profile as a function of $\Delta G_{\text{GRSV}}^{[0.02,0.3]}$ when the theoretical scale is set to $\mu = p_T$, $p_T/2$, and $2p_T$.

the shape of $\Delta g(x)$ were also varied. While this results in different GRSV χ^2 profiles, the $\Delta\chi^2 = 1$ and 9 constraints are consistent. The $\Delta G_{\text{GRSV}}^{[0.02,0.3]}$ values at the χ^2 minimum for each parametrization are between 0.1 and 0.2, and are listed in Table I. At $\Delta\chi^2 = 9$, the profiles of all parametrizations are consistent with $-0.7 < \Delta G_{\text{GRSV}}^{[0.02,0.3]} < 0.5$, indicating that the data are primarily sensitive to the size of $\Delta G_{\text{GRSV}}^{[0.02,0.3]}$, while remaining largely insensitive to the shape of $\Delta g(x)$.

The cross section for π^0 production has been presented [8] and compared with NLO pQCD expectations with the theoretical scales (factorization, fragmentation, and renormalization) in the calculation all set equal to $\mu = kp_T$ with $k = 1$. The calculation agreed with the results within the sizable theoretical uncertainties in the choice of scale, which were estimated by varying k up and down by a factor of 2. As we rely on NLO pQCD to extract $\Delta G_{\text{GRSV}}^{[0.02,0.3]}$ from the measured $A_{\text{LL}}^{\pi^0}$, we must consider the effect of this uncertainty. Figure 4 shows the change in the $\Delta G_{\text{GRSV}}^{[0.02,0.3]}$ constraint when varying k in the A_{LL} calculation in the GRSV parametrization. This variation leads to an additional uncertainty of $\pm 0.1_{(-0.4)}^{(+0.1)}$ at $\Delta\chi^2 = 1$ ($\Delta\chi^2 = 9$). Thus, including these theoretical uncertainties, we find $\Delta G_{\text{GRSV}}^{[0.02,0.3]} = 0.2 \pm 0.1(\text{stat}) \pm 0.1(\text{syst})_{-0.4}^{+0.0} \times (\text{shape}) \pm 0.1(\text{scale})$.

We have presented results for $A_{\text{LL}}^{\pi^0}$ from 2006 which are consistent with zero. We extract $\Delta G_{\text{GRSV}}^{[0.02,0.3]}$ after combining with the 2005 results [8]. Using four parametrizations of $\Delta g(x)$, we find a shape independent constraint of $-0.7 < \Delta G_{\text{GRSV}}^{[0.02,0.3]} < 0.5$ at $\Delta\chi^2 = 9$ ($\sim 3\sigma$). The theoretical scale induced uncertainty is small for positive values of $\Delta G_{\text{GRSV}}^{[0.02,0.3]}$, but is sizable for negative values. Future measurements will be required to measure $\Delta g(x)$ for $x < 0.02$ where large uncertainty remains [11] and which may still contribute a significant amount of the proton spin. The quark spin contribution was well constrained by pDIS and our results begin to significantly constrain the gluon spin contribution.

We thank the staff of the Collider-Accelerator and Physics departments at BNL for their vital contributions, and Marco Stratmann and Werner Vogelsang for communications. We acknowledge support from the Office of Nuclear Physics in the DOE Office of Science; NSF; and a sponsored research grant from Renaissance Technologies (U.S.); MEXT and JSPS (Japan); CNPq and FAPESP (Brazil); NSFC (China); MSMT (Czech Republic); IN2P3/CNRS and CEA (France); BMBF, DAAD, and AvH (Germany); OTKA (Hungary); DAE (India); ISF (Israel); KRF and KOSEF (Korea); MES, RAS, and FAAE (Russia); V.R. and KAW (Sweden); U.S. CRDF for the FSU; U.S.-Hungary Fulbright; U.S.-Israel BSF.

*PHENIX Spokesperson.

jacak@skipper.physics.sunysb.edu

[†]Deceased.

- [1] J. Ashman *et al.*, Nucl. Phys. **B328**, 1 (1989).
- [2] A. Airapetian *et al.*, Phys. Rev. D **75**, 012007 (2007).
- [3] V. Y. Alexakhin *et al.*, Phys. Lett. B **647**, 8 (2007).
- [4] B. Jäger, A. Schäfer, M. Stratmann, and W. Vogelsang, Phys. Rev. D **67**, 054005 (2003).
- [5] J. Adams *et al.*, Phys. Rev. Lett. **92**, 171801 (2004).
- [6] B. I. Abelev *et al.*, Phys. Rev. Lett. **97**, 252001 (2006).
- [7] S. S. Adler *et al.*, Phys. Rev. D **71**, 071102 (2005).
- [8] A. Adare *et al.*, Phys. Rev. D **76**, 051106 (2007).
- [9] S. S. Adler *et al.*, Phys. Rev. Lett. **93**, 202002 (2004).
- [10] S. S. Adler *et al.*, Phys. Rev. D **73**, 091102 (2006).
- [11] D. de Florian, R. Sassot, M. Stratmann, and W. Vogelsang, Phys. Rev. Lett. **101**, 072001 (2008).
- [12] M. Glück, E. Reya, M. Stratmann, and W. Vogelsang, Phys. Rev. D **63**, 094005 (2001).
- [13] J. Bluemlein and H. Bottcher, Nucl. Phys. **B636**, 225 (2002).
- [14] E. Leader, A. V. Sidorov, and D. B. Stamenov, Phys. Rev. D **73**, 034023 (2006).
- [15] T. Gehrmann and W. J. Stirling, Phys. Rev. D **53**, 6100 (1996).
- [16] M. Stratmann (private communication).
- [17] S. S. Adler *et al.*, Phys. Rev. D **74**, 072002 (2006).
- [18] L. Aphecetche *et al.*, Nucl. Instrum. Methods Phys. Res., Sect. A **499**, 521 (2003).
- [19] S. S. Adler *et al.*, Phys. Rev. Lett. **91**, 241803 (2003).
- [20] M. Allen *et al.*, Nucl. Instrum. Methods Phys. Res., Sect. A **499**, 549 (2003).
- [21] Y. Fukao *et al.*, Phys. Lett. B **650**, 325 (2007).
- [22] M. Allen *et al.*, Nucl. Instrum. Methods Phys. Res., Sect. A **470**, 488 (2001).
- [23] J. Pumplin *et al.*, J. High Energy Phys. 07 (2002) 012.
- [24] D. de Florian, R. Sassot, and M. Stratmann, Phys. Rev. D **75**, 114010 (2007).
- [25] A. D. Martin, R. G. Roberts, W. J. Stirling, and R. S. Thorne, Eur. Phys. J. C **28**, 455 (2003).
- [26] B. A. Kniehl, G. Kramer, and B. Potter, Nucl. Phys. **B582**, 514 (2000).